crystals

MDPI

Article

Study of the Unstable Rotational Dynamics of a Tor-Fullerene Molecular System

Vladislav Borodin [1], Mikhail Bubenchikov [2], Alexey Bubenchikov [2], Dmitriy Mamontov [2,*], Sergey Azheev [2] and Alexandr Azheev [2]

[1] Gazprom Transgaz Tomsk LLC, Tomsk 634050, Russia
[2] Department of Mathematics and Mechanics, National Research Tomsk State University, Tomsk 634050, Russia
* Correspondence: orevaore@mail.ru; Tel.: +7-9521526410

Abstract: This work is devoted to modeling the dynamics of large molecules. The key issue in modeling the dynamics of real molecular systems is to correctly represent the temperature of the system using the available theoretical tools. In most works on molecular dynamics, vibrations of atoms inside a molecule are modeled with enviable persistence, which has nothing to do with physical temperature. These vibrations represent the energy internal to the molecule. Therefore, it should not be present in problems in the dynamics of inert molecular systems. In this work, by means of classical mechanics, it is shown that the simplest system containing only three molecular bodies, due to multiple acts of pair interactions of these bodies, reproduces the temperature even in an extremely complex unstable motion of the system. However, at the same time, it is necessary to separate the stochastic part of the movement from the deterministic one. Calculations also show that translational fluctuations in the motion of molecules make the greatest contribution to temperature. The contribution of rotational energy to the total energy of fluctuation motions is small. It follows from these results that the thermal state of the system is determined only by the translational temperature. The latter, in turn, opens up possibilities for a simplified description of many complex systems composed of carbon molecules such as fullerenes and nanotori.

Keywords: molecular dynamics; mathematical modeling; nanomaterials; nanotori; fullerene; CNT; carbon nanotube; C60

check for updates

Citation: Borodin, V.; Bubenchikov, M.; Bubenchikov, A.; Mamontov, D.; Azheev, S.; Azheev, A. Study of the Unstable Rotational Dynamics of a Tor-Fullerene Molecular System. *Crystals* **2023**, *13*, 181. https://doi.org/10.3390/cryst13020181

Academic Editors: Walid M. Daoush, Fawad Inam, Mostafa Ghasemi Baboli and Maha M. Khayyat

Received: 20 November 2022
Revised: 13 January 2023
Accepted: 14 January 2023
Published: 20 January 2023

Copyright: © 2023 by the authors. Licensee MDPI, Basel, Switzerland. This article is an open access article distributed under the terms and conditions of the Creative Commons Attribution (CC BY) license (https://creativecommons.org/licenses/by/4.0/).

1. Introduction

The study of complex movements of carbon molecules in molecular systems is important for the development of nanorobotics. Such equipment can perform a wide range of functions in long-term space flight conditions. This technique is already being used in a number of medical applications. Typical fragments of molecular structures are carbon nanotori and fullerenes since they have a rigid framework structure. Previous reports [1–5] are devoted to the study of the properties of molecular complexes containing standard fullerenes. These studies found that C60 fullerenes can effectively increase the mechanical strength of SWNTs, by acting as a "barrier" to prevent radial deformation and as an inner wall in a double-walled carbon nanotube, as well as the study of the current–voltage characteristics of a system consisting of fullerene and two-carbon nanotubes. Ref. [6] analyzed the interaction of fullerenes with a graphene ribbon accessible to a groove. Based on this interaction, an oscillator was developed. Ref. [7] investigated the transfer of electrons through a carbon molecular transition, a transition from C_{60} molecules attached to a metal concentrate CNT, leading to a coherent regime. It has been shown that the number of contact points between electrodes and a molecule can play an important role in electric transport. Ref. [8] analyzed the features of the interaction of C_{60} with graphite. This article explores the various mechanisms by which C_{60} can be encapsulated in SWNT. Ref. [9], using molecular dynamics simulations, showed that an electric field applied to a @C_{60}

ion inside a water-filled carbon nanotube can pump water with excellent efficiency. A fully controlled nanoelectromechanical device capable of pumping liquids at the nanoscale is proposed. Ref. [10] studied the interaction of a fullerene with a CNT beam. Based on this study, a change in the oscillation frequency is shown depending on the geometric parameters. Ref. [11] developed a multiscale method for predicting the Young's modulus of polymer nanocomposites reinforced with fullerenes (FRPN) and proposed a polymer nanocomposite with a poly(methyl methacrylate) matrix and reinforcing elements in the form of C_{60}. In the study by [12], by analyzing the changes in intermediates and products formed during thermal conversion, the main dependence of the pyrolysis and graphitization of fullerenes on temperature and carbon sources was revealed. It has been found that a higher temperature significantly accelerates the pyrolysis of fullerenes and produces a huge variety of porous carbon products. Ref. [13] studied the possible formation of methane hydrate containing 8, 10, 12, 14, 16, 18, and 20 water molecules into fullerene C_{240} was studied for the first time. After placing a methane molecule in a fullerene containing 20 water molecules, the closed water molecules formed an almost complete dodecahedron shape, and the methane molecule ended up in the center of the dodecahedron. This is the most ordered polygonal structure of methane clathrate, formed into C_{240} fullerene, which is more stable than other clathrate structures. Ref. [14] studied the mechanical and thermodynamic properties of cis-PI-fullerene (C_{60}) composites and achieved the simulation of coarse-grained molecular dynamics (MD) of cis-PI-C_{60} composites with different concentrations of fullerenes. It was found that the density, bulk modulus, thermal expansion, heat capacity and Tg of NR composites increase with increasing C_{60} concentration. The presence of C_{60} led to a slight increase in the interterminal distance and the radius of rotation of the cis-PI chains. The contribution of C_{60} and cis-PI interfacial interactions led to an increase in the bulk moduli of the composites. Ref. [15] studied how the soot core is exposed to polycyclic aromatic hydrocarbons and then grows due to the condensation of polycyclic aromatic hydrocarbons. A nonbonding interaction between polycyclic aromatic hydrocarbons and carbon black has been studied using the distribution of free energy during dimerization and condensation. Ref. [16] are also using molecular dynamics simulations to evaluate the electrical interactions of fullerenes with ions contained in water. The results indicate a smaller chemical shift $\delta(^{13}C)$ and a more intense electronic transition band for fully polarized C_{60} in solution. In [17–21], studies of fullerenes and carbon nanotori by molecular dynamics methods are presented. Extensive results of computational molecular dynamics of various structures were obtained, and interaction potentials and mathematical models were developed.

In the present work, the state of the nanothory system and two fullerenes inside are studied via molecular dynamics methods. It is quite possible to call such a system compact, since molecular objects are together for an arbitrarily long time. The purpose of this work is to define the molecular temperature as an average stochastic characteristic determined by multiple impacts of fullerenes on a nanotorus. The existence of such a temperature indicates the presence of dynamic equilibrium in the system.

2. Computational and Theoretical Models

Models of the dynamics of large molecules are used in the work. This means that individual fragments of the molecular system move as non-deformable molecular shells, interacting with each other and, perhaps, with external electromagnetic fields. At the same time, the interaction of two molecular objects with each other is the total result of the interaction of each atom of one molecular body with all atoms of another. There are three molecular bodies in the case under consideration: a nanotorus and two fullerenes. The rotational motion of each of these bodies can be described using vector equations for a change in the kinetic moment (moment of momentum) for each of these bodies:

$$\frac{d\boldsymbol{K}_1}{dt} = \boldsymbol{L}_1, \ \frac{d\boldsymbol{K}_2}{dt} = \boldsymbol{L}_2, \ \frac{d\boldsymbol{K}_3}{dt} = \boldsymbol{L}_3. \tag{1}$$

where $\boldsymbol{K_1}$, $\boldsymbol{K_2}$, $\boldsymbol{K_3}$ are the kinetic moments of individual bodies; $\boldsymbol{L_1}$,$\boldsymbol{L_2}$,$\boldsymbol{L_3}$—moments of forces acting on this body from the remaining two molecular bodies. In this case, due to the pairing of van der Waals interactions and the absence of external forces:

$$\boldsymbol{L}_1 + \boldsymbol{L}_2 + \boldsymbol{L}_3 = 0. \tag{2}$$

Then, the combination of Equation (1) can be written as follows:

$$\frac{d}{dt}(\boldsymbol{K}_1 + \boldsymbol{K}_2 + \boldsymbol{K}_3) = 0. \tag{3}$$

From (3), we find by integration:

$$\boldsymbol{K}_1 + \boldsymbol{K}_2 + \boldsymbol{K}_3 = \boldsymbol{C}, \tag{4}$$

Here, $\boldsymbol{C}$ is a vector constant. Thus, if no external forces act on a molecular system, then its total angular momentum retains its value both in magnitude and direction.

The angular momentum of the first molecular body $\boldsymbol{K}_\mathrm{j}$ is the product of the tensor of inertia $\hat{\boldsymbol{J}}_j$, and the column vector of the instantaneous angular velocity of this body $\boldsymbol{\omega_j}$:

$$\boldsymbol{K}_1 = \hat{\boldsymbol{J}}_j \boldsymbol{\omega}_j. \ (j = 1, 2, 3). \tag{5}$$

Further omitting the index that determines the particular body for the tensor of inertia, the following can be written:

$$\hat{\boldsymbol{J}} = \begin{pmatrix} m\sum\left(y_i^2 + z_i^2\right) & -m\sum x_i y_i & -m\sum x_i z_i \\ -m\sum y_i x_i & m\sum\left(x_i^2 + z_i^2\right) & -m\sum y_i z_i \\ -m\sum x_i z_i & -m\sum y_i z_i & m\sum\left(x_i^2 + y_i^2\right) \end{pmatrix}. \tag{6}$$

where the summation is over the number of atoms that make up the molecule; x_i,y_i,z_i are the coordinates of the i-th atom; m is the mass of the carbon atom. Thus, the components of the inertia tensor of a molecular body are the summation (over the entire number of atoms) of the quadratic functions of the coordinates of the individual atoms that make up the molecule under consideration. The coordinates of all nodes of the molecular body are calculated using the following formula:

$$\frac{d\boldsymbol{r}_i}{dt} = \boldsymbol{\omega} \times \boldsymbol{r_i} + \boldsymbol{v_c} \ \left(i = \overline{1, N}\right). \tag{7}$$

where $\boldsymbol{r_i}$ = (x_i,y_i,z_i); N is the number of atoms that make up the molecular body; ω is the instantaneous angular velocity vector of the considered molecule; $\boldsymbol{v_c}$ is the velocity of the center of mass of this molecule. The last relation expresses the theorem of the addition of velocities in the complex motion of a material point, namely, together with the center of mass and around it. For the velocities of the centers of mass of all molecular bodies participating in the interaction, the equations of motion of their centers of mass are valid:

$$\boldsymbol{F}_1 = M_1 \frac{d\boldsymbol{v}_{c1}}{dt}, \ \boldsymbol{F}_2 = M_2 \frac{d\boldsymbol{v}_{c2}}{dt}, \ \boldsymbol{F}_3 = M_3 \frac{d\boldsymbol{v}_{c3}}{dt}. \tag{8}$$

where M_1 is the nanotorus mass, M_2, M_3 are the fullerene masses, $\boldsymbol{F_1}$ is the sum of all forces acting on the nanotori atoms from the fullerene atoms; $\boldsymbol{F_2}$ and $\boldsymbol{F_3}$ are the total forces of action on the fullerene under consideration from the nanotori and the remaining fullerene. As can be seen from the written relations, the center of mass of the molecule will move at a speed noticeably lower than that of fullerenes since its mass is much greater. In this case, each atom–atom interaction between nodes belonging to different molecular bodies is determined by the gradient of the interaction potential used. The origin of coordinates is chosen at the center of mass of the system. In this case, the components of the tensor of inertia will be calculated by Equation (6) and will be functions of time. The

new position of the molecular body in space will be determined by the coordinates of all its points, i.e., coordinates of carbon atoms. If the molecular body is large, then the number of calculated coordinates can be reduced by collecting atoms at the center of mass of some representative fragment. As can be seen from the above description, there is no need to use the Euler angles, as well as the Euler kinematic relations, which have a coordinate singularity. All calculations were carried out according to the Runge–Kutta scheme [22] of the fourth order of accuracy with a constant time step $\Delta t = 10^{-6}$ ns. The accuracy of the calculations was checked by performing the balance of the total energy of the system and amounted to 10^{-8} relative units. The calculated kinetic energy was related to the initial potential energy of the interaction of molecular bodies. The LJ potential of atom–atom interactions was used in the calculations. This is a classical potential: attraction–repulsion, which has two parameters of interaction: ε is the depth of the potential well, and σ is the radius of influence of the interaction. Leaving σ unchanged (0.34 nm for carbon atoms), we select the depth of the potential well in such a way that the vibration energy of the bodies participating in the movement corresponds to a certain temperature, in this case, room temperature T = 300 K (ε/k = 5.1 K, where k is Boltzmann constant). The vibrations of carbon atoms in the molecular bodies under consideration must correspond to this temperature. In this case, however, due to the small mass of atoms and strong *C-C* bonds, they have a higher frequency and a significantly lower amplitude. Their inclusion in the consideration does not affect the nature of movements on larger scales. Therefore, they remain small-scale and high-frequency, forming the background against which larger-scale molecular events unfold.

3. Results

For solving the system of such equations, step-by-step integration schemes of the Runge–Kutta class of the fourth order with a constant time step $\Delta t = 10^{-7}$ ns are used. All calculations were carried out using the software developed by the authors according to the scheme proposed in this work for determining the rotations of molecular bodies in space.

Figure 1 presents the case of rotation of the torus with an initial angular velocity of $\omega_x^0 = 150\ ns^{-1}$, $\omega_y^0 = \omega_z^0 = 0$. In this case, the fullerenes are located diametrically opposite on the (*oy*) axis and are fixed on the axial circumference of the torus. The red line in this figure is the trajectory of one of the peripheral carbon atoms that does not lie on the (*ox)* axis and has a y-coordinate value close to the outer radius of the torus. This line demonstrates somersaults of the considered molecular structure during its rotation around an axis with an intermediate moment of inertia (*oy* axis), i.e., demonstrates the instability of Louis Poinsot [23–25]. The *(oz*) axis is directed perpendicular to the initial position of the torus plane. In what follows, the motion of the molecular structure under consideration is analyzed in the absolute frame of reference thus introduced.

In addition, in this article, the rotation of a tor-fullerene molecular system is considered. Thus, we compare the case of fullerenes having internal freedom with the case of fullerenes maximally separated and fixed inside the torus. The nanotorus is composed of 2000 carbon atoms and has an inner radius R_1 = 0.3 nm, R_2 = 1.9 nm (Figure 2). It contains standard C_{60} fullerenes. In all variants, the fullerenes are maximally spaced at the initial moment, and the rotation is carried out around an axis lying in the plane of the torus and passing perpendicular to the straight line connecting the centers of mass of the fullerenes. In the case of loose fullerenes, the rotation of the system around an axis with an intermediate moment of inertia forms orbital displacements of fullerenes along the axis of the nanotorus channel.

The data are reduced to a moving frame of reference with coordinate axes lying in the rotating plane of the torus. It turned out that somersaults of the torus induce reciprocating movements of fullerenes along the curvilinear axis of the torus. Moreover, the center of such oscillations shifts in a certain direction. The direction of axial displacement of buckyballs is determined by the right hand rule. If the vector of the initial angular velocity of the molecular structure enters the palm of the right hand, and the moved thumb is perpendicular to the plane of the torus and points to the vector of its angular rotation, and

then the index finger shows in which direction the fullerenes move. The red line in the center of Figure 2 shows the trajectory of the center of mass of the nanotorus in this case. The center of mass of the torus is displaced due to the movement of fullerenes; however, the center of mass of the entire torus–fullerene structure remains immobile. The case of the rotation of such a system, which has some freedom of movement for fullerenes inside the torus, demonstrates one of the options for the transition of the rotational motion of the system into the translational motion of fullerenes along the circle, which is the axial line of the torus channel. It should be noted that in this case, fullerenes receive rotations in intensity significantly exceeding their initial values. These metamorphoses are associated with a decrease in the rotational energy of the frame body, which has a significantly larger mass than fullerenes. These peculiarities of motion are associated with a decrease in the rotational energy of the frame body, which has a much larger mass than fullerenes. The nature of the angular vibrations of fullerenes is shown in Figure 3.

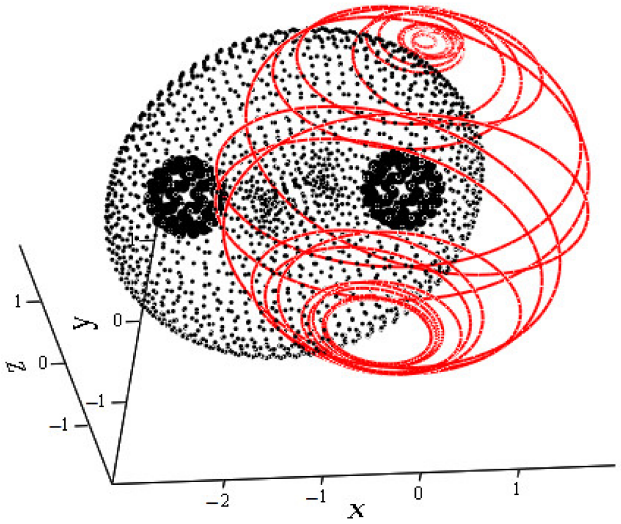


Figure 1. Unstable rotation of a tor-fullerene molecular structure. The red line shows the trajectory of one of the nanotorus atoms.

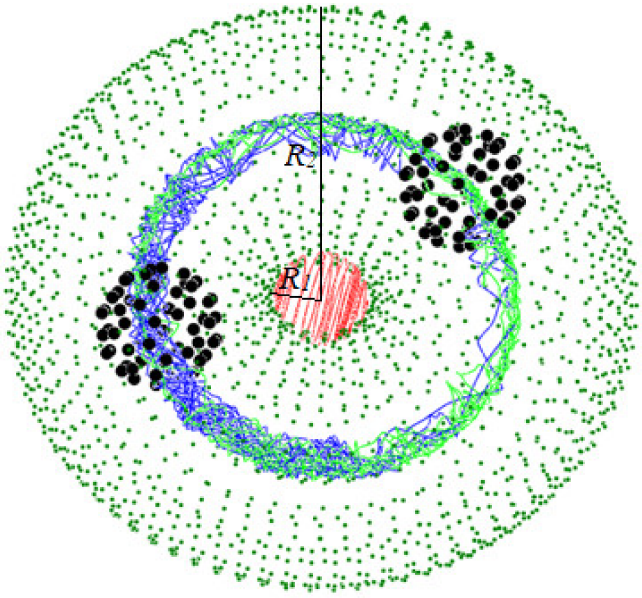


Figure 2. Orbital motion of fullerenes. In the center of the figure, the trajectory of the center of mass of the nanotorus; inside the torus, the trajectory of the centers of mass of fullerenes.

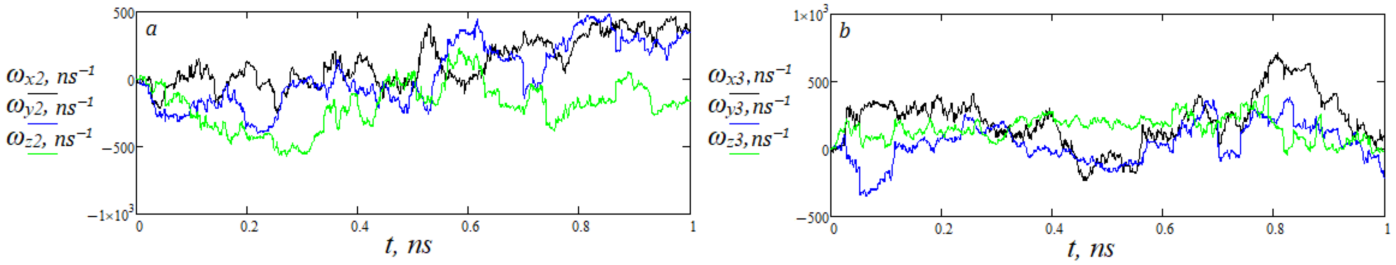


Figure 3. Projections of the angular velocities of fullerenes. (**a**)—the case of "frozen" fullerenes. (**b**)—case of free fullerenes.

Figure 3 shows that the frequencies of angular vibrations of fullerenes are at least 3 times higher than the main frequency of rotation of the body part of the molecular struc-ture. Next, we compare two variants of calculations of the motion of the molecular struc-ture under consideration. Figure 3a refers to the case of pinned fullerenes. Figure 3b variant, fullerenes can move freely in the accessible zones of the inner space of the torus.

Figures 4–6 show the projections of the angular velocities of the torus in these cases. It can be seen that the rotation of a single structure is periodic at the beginning of the movement. In the second case, some quasi-periodic motion is established on a time interval of 1 ns. Figure 4 shows what part of the initial rotational energy of the torus is converted into the kinetic energy of fullerenes. As can be seen from Figures 4 and 6, in the case of "frozen" fullerenes, one can clearly distinguish bi-oscillations, which are determined by the presence of two frequencies—the initial frequency of rotations of the system and the frequency of somersaults by V. Dzhanibekov [26].

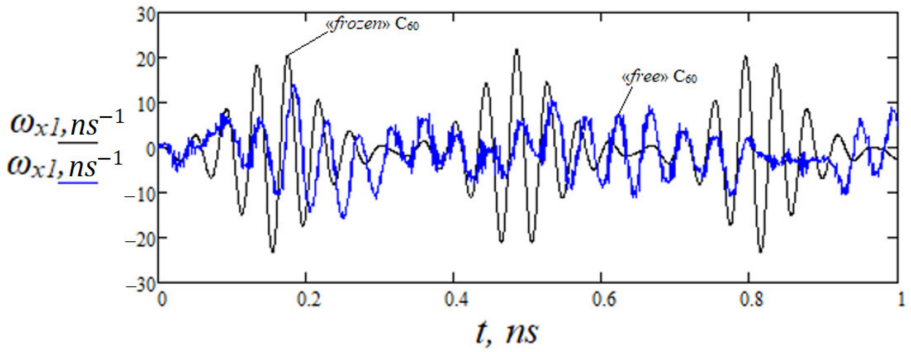


Figure 4. Comparison of rotations of two systems with free and "frozen" fullerenes.

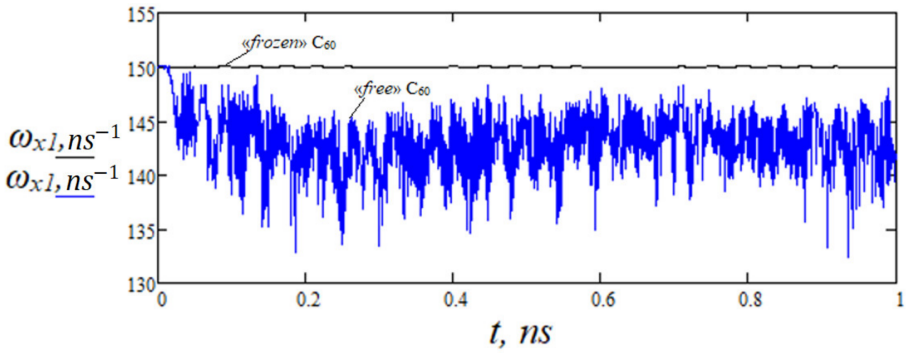


Figure 5. Change in time of the *y*-component of the angular velocity of the nanotorus.

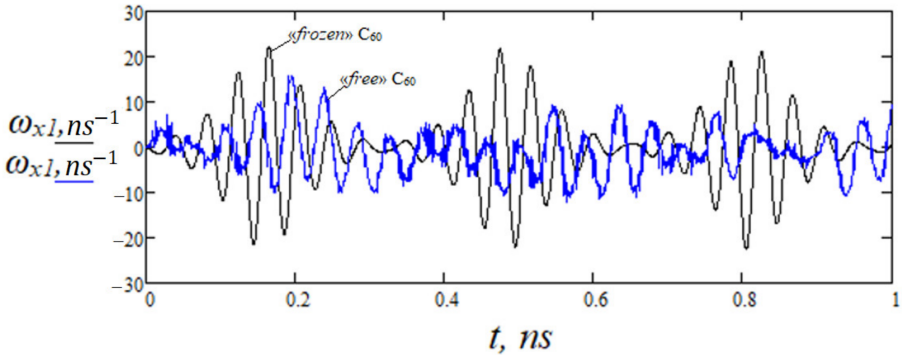


Figure 6. Distribution of the *z*-component of the angular velocity of the nanotorus.

Figure 7 shows the total angular frequency modulus of the nanotorus with "frozen" fullerene. The highest peaks on this graph show "Dzhanibekov flips", and the time between peaks is the period with which these somersaults are made.

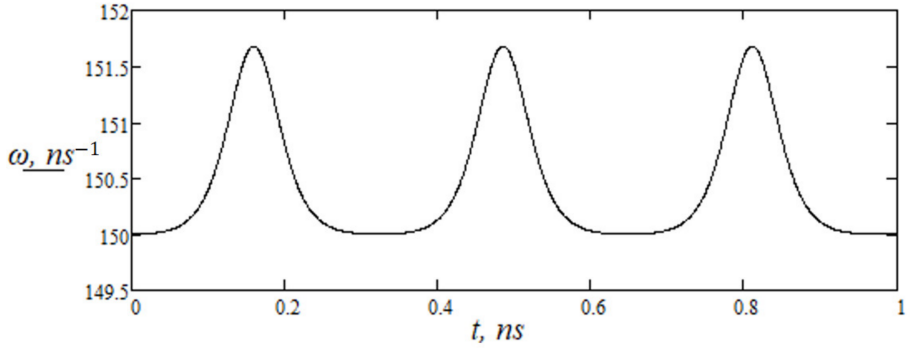


Figure 7. Module of angular velocity of nanotorus with "frozen" fullerene.

Since the inertial rotation of the molecular system is considered, the vector of the angular momentum of the entire system $\boldsymbol{K}$ remains constant during the entire time of motion. There is a non-moving plane perpendicular to this vector, where in the case of one body, the vector of the instantaneous angular velocity of this body will draw a complete picture of the motion instability. This plane is called the Poinsot plane, and the trajectory of the end of the instantaneous angular velocity vector on this plane is called the herpoloid [23]. In the case of several bodies (a torus plus two fullerenes), the Poinsot plane also exists, but the end of the angular velocity vector of any of the existing bodies will not slide along this plane. Nevertheless, the behavior of the projection onto this plane of the vector of the instantaneous angular velocity of the frame body is of interest, i.e., the molecular torus, as a body having a significantly larger mass in comparison with other structural elements.

Figure 8 shows the trajectory of the end of the instantaneous angular velocity vector of a nanotori with fullerenes "frozen" into it. As can be seen from the presented figure, the herpoid in this case is a fairly smooth curve. The general view of the drawing resembles a bud of an unopened flower. The herpoid of a single body with different values of the axial moments of inertia is always a petal structure. It is just that with such a slight difference in the moments of inertia, as in the case under consideration, the petals in the bud are too wide and they are tightly packed. With a more significant difference in the axial moments of inertia, a chamomile herpoid design can be obtained. In any case, if the molecular body is uniform, then the end of the vector of its instantaneous angular velocity moves step by step in one direction along the herpoloid.

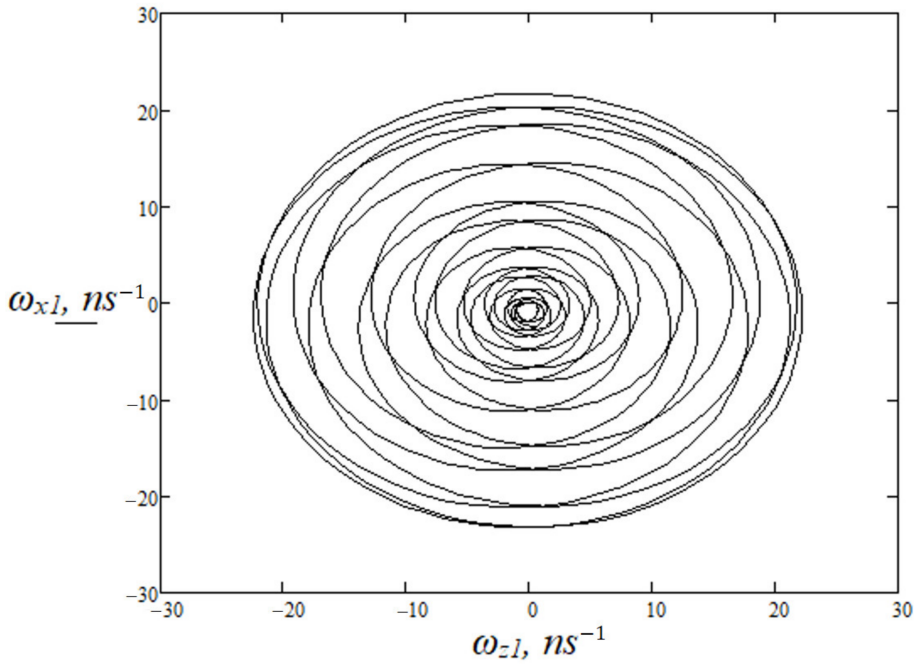


Figure 8. Herpoloid torus with "frozen" fullerenes.

Figure 9 shows what happens to the herpolody when fullerenes are able to move inside the torus space. The motion along the herpoid takes on a reciprocating character, although globally, it remains unidirectional. The kinks on the herpoid are associated with the reciprocating motion of fullerenes inside the torus.

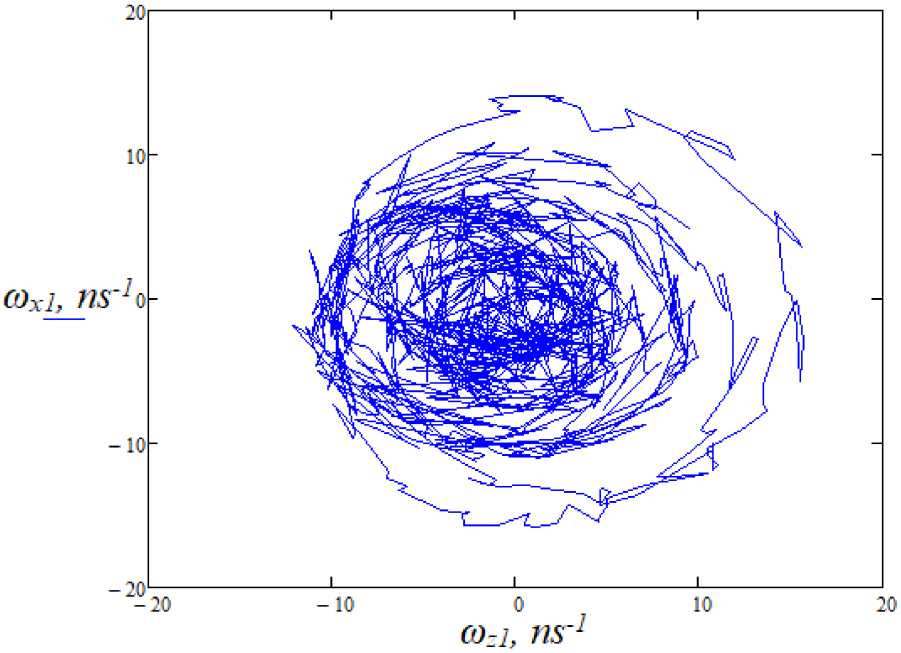


Figure 9. Herpoid composite molecular structure with freely moving fullerenes.

4. Discussion

Despite the fact that the case described by Louis Poinsot is an example of the instability of motion, it is characterized by a regular rotation of a molecular object with strictly periodic flips around the axis with a minimum moment of inertia. Such movement can rightly be attributed to the class of deterministic processes. Calculations show that the interactions of two molecular objects already lead to the appearance of irregular oscillations in this simplest system. All this is a sign of the manifestation of stochastic properties. The two fullerenes considered in this paper inside the nanotorus have random angular rotations, as well as random approaches of fullerenes to the wall. However, under the conditions of the considered problem, the transversal displacements of fullerenes inside the torus turned out to be deterministic. To determine the direction of these movements, the authors adapted the right hand rule. It is known that somersaults of an object rotating by inertia have a certain direction of flips. These flips generate displacements of fullerenes in a strictly defined direction along the axial circumference of the torus. However, these movements are defined only in a global sense, since they have a local reciprocating character. Thus, the system demonstrates stochastic properties all the time of movement. Even fullerenes of small mass create disturbances that greatly loosen the motion of the nanotorus. In this regard, the instantaneous axis of rotation of the nanotorus ceases to smoothly and monotonously change its direction in space. The motion of the entire system becomes largely stochastic. However, it is still possible to single out a deterministic part of it. In this regard, the method of comparing the main variant with the motion of a torus with "frozen" fullerenes turned out to be useful. This case made it possible to isolate the second frequency in the oscillations of the nanotorus due to its flips around the axis with the minimum value of the moment of inertia. Thus, the temperature of a system consisting of a small number of bodies is considered from a not quite classical angle. The molecular dynamics of a very interesting system consisting of fullerenes were also considered. Despite the fact that both nanotori and fullerenes themselves are of great scientific interest and are being studied quite closely [26,27], and similar container-like nanostructures are already proposed for use [28,29], even the theoretical side of these issues has not been fully studied. In this case, any of the found effects or mechanisms can form the basis of various technologies.

5. Conclusions

The interaction of a large nanotorus molecule with a standard C60 fullerene, which makes up only 3% of the mass of the body of the torus, leads to the appearance of thermal motions of both the nanotorus itself and the fullerene contained in it. Moreover, the average values of the energies of random displacements distributed over the six degrees of freedom of each of the molecular bodies are extremely close. This indicates a rapidly emerging equilibrium in the system. In the case of a nanotorus plus two fullerenes considered here, due to multiple impacts on the inner wall of the nanotorus, the equality of the energies of rotational fluctuation displacements of fullerenes with the energy of their translational fluctuations occurs, which ultimately ensures the equality of rotational and vibrational temperatures. The foregoing makes it possible to conclude that there is a single temperature in the system due to the movement of molecular bodies.

Author Contributions: Data curation, V.B.; funding acquisition, M.B.; investigation, A.B.; methodology, M.B., A.B., S.A. and A.A.; project administration, M.B.; resources, M.B.; software, D.M.; supervision, M.B.; validation, A.B.; visualization, D.M.; writing—original draft, D.M. and A.A.; writing—review and editing, A.B. and S.A. All authors have read and agreed to the published version of the manuscript.

Funding: This research was funded by presidential grant MD 4273.2022.1.1.

Data Availability Statement: Not applicable.

Conflicts of Interest: The authors declare no conflict of interest.

References

1. Wu, C.-D.; Fang, T.-H.; Chan, C.-Y. A molecular dynamics simulation of the mechanical characteristics of a C60-filled carbon nanotube under nanoindentation using various carbon nanotube tips. *Carbon* **2011**, *49*, 2053–2061. [CrossRef]
2. Tu, G.-Y.; Guo, D.-P.; Li, B.-R.; Zhang, H.-L. Transport properties and mechanism of C60 coupled to carbon nanotube electrode. *Phys. B Condens. Matter* **2011**, *406*, 2138–2142. [CrossRef]
3. Kang, J.W.; Hwang, H.J. Comparison of C60 encapsulations into carbon and boron nitride nanotubes. *J. Phys. Condens. Matter* **2004**, *16*, 3901. [CrossRef]
4. Shokri, A.; Nikzad, S. Electrical transport properties of a CNT/C60/CNT hybrid junction with closed end CNT leads using Green's function method. *Eur. Phys. J. B* **2013**, *86*, 22. [CrossRef]
5. Zhou, L.; Zhu, B.E.; Pan, Z.Y.; Wang, Y.X.; Zhu, J. Reduction of the buckling strength of carbon nanotubes resulting from encapsulation of C60 fullerenes. *Nanotechnology* **2007**, *18*, 275709. [CrossRef]
6. Kang, J.W.; Lee, K.W. Molecular dynamics study on the C60 oscillator in a graphene nanoribbon trench. *J. Korean Phys. Soc.* **2014**, *65*, 185–189. [CrossRef]
7. Shokri, A.A.; Nikzad, S. Topology effects of interface and gate voltage on electrical transport through the CNT/C60/CNT junction using the Green's function method. *J. Appl. Phys.* **2011**, *110*, 024303. [CrossRef]
8. Ulbricht, H.; Moos, G.; Hertel, T. Interaction ofC60with Carbon Nanotubes and Graphite. *Phys. Rev. Lett.* **2003**, *90*, 095501. [CrossRef]
9. Farimani, A.B.; Heiranian, M.; Aluru, N.R. Nano-electro-mechanical pump: Giant pumping of water in carbon nanotubes. *Sci. Rep.* **2016**, *6*, 26211. [CrossRef]
10. Ansari, R.; Sadeghi, F.; Alipour, A. Oscillation of C60 Fullerene in Carbon Nanotube Bundles. *J. Vib. Acoust.* **2013**, *135*, 051009. [CrossRef]
11. Izadi, R.; Nayebi, A.; Ghavanloo, E. Combined molecular dynamics–micromechanics methods to predict Young's modulus of fullerene-reinforced polymer composites. *Eur. Phys. J. Plus* **2021**, *136*, 816. [CrossRef]
12. Li, S.; Bian, F.; Meng, X.; Zhai, D.; Yang, H.; Qin, G. Ring structure characterization of nanoporous carbon materials prepared by thermal conversion of fullerenes: Insights from ReaxFF molecular dynamics simulations. *Carbon* **2021**, *189*, 484–492. [CrossRef]
13. Abbaspour, M.; Akbarzadeh, H.; Salemi, S.; Tahami, S.F. Formation of methane clathrates into fullerene: A molecular dynamics study. *J. Mol. Liq.* **2022**, *367*, 120587. [CrossRef]
14. Kitjanon, J.; Khuntawee, W.; Phongphanphanee, S.; Sutthibutpong, T.; Chattham, N.; Karttunen, M.; Wong-Ekkabut, J. Nanocomposite of Fullerenes and Natural Rubbers: MARTINI Force Field Molecular Dynamics Simulations. *Polymers* **2021**, *13*, 4044. [CrossRef] [PubMed]
15. Yuan, H.; Kong, W.; Xia, J. Steered molecular dynamics and stability analysis on PAH dimerisation and condensation on fullerene and soot surfaces. *Phys. Chem. Chem. Phys.* **2021**, *23*, 19590–19601. [CrossRef] [PubMed]
16. Cardoso, W.B.; Colherinhas, G. Fullerene C60 spectroscopy in [BMIM][PF6] ionic liquid: Molecular dynamics study using polarization effects. *J. Mol. Struct.* **2021**, *1250*, 131887. [CrossRef]
17. Lun-Fu, A.V.; Bubenchikov, A.M.; Ovchinnikov, V.A. Numerical study of rotational dynamics of carbon nanotori during intermolecular interaction. *J. Phys. Conf. Ser.* **2022**, *2211*, 012004. [CrossRef]
18. Lun-Fu, A.; Bubenchikov, M.; Bubenchikov, A.; Mamontov, D.; Borodin, V. Interaction of molecular tori in columnar structures. *J. Phys. Condens. Matter* **2022**, *34*, 125101. [CrossRef]
19. Bubenchikov, M.; Mamontov, D.; Ovchinnikov, V. Studying the possibility of using fullerenes inside carbon nanotubes as a molecular engine. *J. Phys. Conf. Ser.* **2022**, *2211*, 012005. [CrossRef]
20. Bubenchikov, A.M.; Bubenchikov, M.A.; Mamontov, D.V.; Chelnokova, A.S.; Chumakova, S.P. Movement of fullerenes and their dimers inside carbon nanotubes. *Full- Nanotub. Carbon Nanostruct.* **2021**, *29*, 803–809. [CrossRef]
21. Bubenchikov, A.M.; Bubenchikov, M.A.; Mamontov, D.V.; Kaparulin, D.S.; Lun-Fu, A.V. Dynamic state of columnar structures formed on the basis of carbon nanotori. *Full- Nanotub. Carbon Nanostruct.* **2021**, *29*, 825–831. [CrossRef]
22. Runge, C. Ueber die numerische Auflösung von Differentialgleichungen. *Math. Ann.* **1895**, *46*, 167–178. [CrossRef]
23. Poinsot, L. *Theéorie Nouvelle De La Rotation Des Corps*; Bachelier: Paris, France, 1834; Volume 1834, pp. 1777–1859.
24. Levi, M. Classical Mechanics with Calculus of Variations, and Optimal Control: An Intuitive Introduction. *Am. Math. Soc.* **2014**, *69*, 1470414449. [CrossRef]
25. Trivisonno, N.; Garelli, L.; Storti, M. The Tennis Racket Theorem, an Analysis of the Intermediate Axis Theorem. *Mecánica Comput.* **2021**, *38*, 1341–1353.
26. Sarapat, P.; Hill, J.M.; Baowan, D. A Review of Geometry, Construction and Modelling for Carbon Nanotori. *Appl. Sci.* **2019**, *9*, 2301. [CrossRef]
27. Shi, J.; Wang, B.; Wang, L.; Lu, T.; Fu, Y.; Zhang, H.; Zhang, Z. Fullerene (C60)-based tumor-targeting nanoparticles with "off-on" state for enhanced treatment of cancer. *J. Control Release* **2016**, *235*, 245–258. [CrossRef] [PubMed]

28. Chernozatonskii, L.A.; Artyukh, A.A.; Demin, V. Quasi-one-dimensional fullerene-nanotube composites: Structure, formation energetics, and electronic properties. *JETP Lett.* **2013**, *97*, 113–119. [CrossRef]
29. Singhai, N.J.; Ramteke, S. Functionalized Carbon Nanotubes: Emerging Applications in the Diverse Biomedical Arena. *Curr. Nanosci.* **2020**, *16*, 170–186. [CrossRef]

Disclaimer/Publisher's Note: The statements, opinions and data contained in all publications are solely those of the individual author(s) and contributor(s) and not of MDPI and/or the editor(s). MDPI and/or the editor(s) disclaim responsibility for any injury to people or property resulting from any ideas, methods, instructions or products referred to in the content.